The protective effects of MSC-EXO against pulmonary arterial hypertension through inhibition of Wnt/BMP signaling pathway

Zhaohua Zhang
Shandong University
Xiaoli Liu
Shandong University
LiLi Ge
Shandong University
Shanshan Zhang
Shandong University
Jue Wang
Shandong University
Wen Jiang
Shandong University
Qian Xin
Shandong University
yun luan (Y_luan@aliyun.com)
shandong university

Research

Keywords: PAH, MSC-EXO, pulmonary vascular remodeling, Wnt5a, BMP

Posted Date: February 19th, 2020

DOI: https://doi.org/10.21203/rs.2.23924/v1

Abstract

Background The aim of the study was to explore the mechanism of mesenchymal human umbilical cord msenchymal stem cells derived exosomes (MSC-EXO) against experimental pulmonary artery hypertension (PAH) pulmonary vascular remodeling .

Methods and results After PAH model was successful established, the animals received tail vein injections of MSC-EXO. Post-operation, the pulmonary artery pressure was measured, and the lung tissues were stained to evaluate the pulmonary vascular remodeling. Our results showed that MSC-EXO could significantly inhibit the pulmonary arterial hypertension, attenuate pulmonary vascular remodeling and lung fibrosis in vivo . Furthermore, the hypoxia-induced pulmonary artery endothelial cell (PAEC) model was used in vitro . Our results showed the expression of CD31, V-Ecadherin, Wnt5a, Wnt11, BMPR2 and Smad1/5/8 were significantly higher, but the expression of alpha smooth muscle actin (a-SMA), β-catenin, cyclin D1 and Smad2/3 were significantly lower in in MSC-EXO administration group then that in MCT or hypoxia group. Moreover, the present study found that BMP signaling suppressed obviously when the cells were transfection with Wnt5a siRNA.

Conclusion In conclusion, these results suggested that MSC-EXO could protect PAH vascular remodeling through regulation of Wnt/BMP signaling pathway.

Introduction

Pulmonary arterial hypertension (PAH) is a life-threatening lung disease is associated with microvascular lost or regenerate damaged[1]. Pulmonary vascular endothelial cells and smooth muscle cells dysfunction caused by pulmonary vascular remodeling, and even the right ventricle hypertrophy and failure is important pathological features of PAH[2, 3]. Abnormal pulmonary vascular cells proliferation which plays a central role in the occurrence and development of PAH[4–6]. Currently, there are a lot of drugs used to improve the clinical symptoms of PAH patients, but, they cannot reverse the pulmonary vascular remodeling process and prevent PAH development, hence, novel approaches are urgently needed.

The pathogenesis of PAH is complicated, the damage of pulmonary artery endothelial cell (PAEC) is a crucial early onset. The proliferation and angiogenesis of PAEC are underlying mechanism for the pathological features. Therefore, Understanding the basis of endothelial angiogenesis molecular and cellular that underlies PAH is important and will help to explore new therapeutic strategies. Wnt5a is one of a member of the Wingless (Wnt), activates non-canonical or canonical Wnt signaling pathways through specific coupling of different receptor. Down-regulation of Wnt5a could promote hypoxia-induced pulmonary vascular smooth muscle cells (PASMC) proliferation [7], loss of Wnt5a could lead to PH via reducing the formation of new vessels[1]. Thus, the production of Wnt5a is likely to become a new way to prevent the small vessel loss in PH.

Work by our group and others have showed that intravenous delivery of mesenchymal stem/stromal cell (MSC) can improve experimental PAH vascular remodeling and right ventricular impairments, however, the mechanism is not very clear. MSC-derived exosomes (MSC-EXO) is one of the main therapeutic vectors, can inhibit PAH and vascular remodeling [8–10]. The ability of MSC-EXO make it a promising potential target for new therapies of PAH. Therefore, the aim of the present study was to observe the protection role of MSC-EXO on PAH-PAEC.

Materials And Methods

Animal model

Forty male Wistar rats weighing 200 g to 250 g were purchased from animal center of Second Hospital of Shandong University. The animal protocols followed the guidelines of the Institutional Animal Care and Use Committee (IACUC) of Shandong University. All rats received humane care in compliance with the Guide for the Care and Use of Laboratory Animals published by the US National Institute of Health.

Isolation and culture of hUCMSC

Isolation of MSCs from human umbilical cord Wharton's Jelly with some modification with some modification [11]. The immunotyping characterization of hUCMSCs occurred at passage 3–4 using human specific antibodies CD34, CD45, CD73, CD90, CD105, HLA-DR (BD Biosciences Pharmingen, San Diego, CA) by a fluorescence-activated cell sorter (FACS, BD FACSAria II). Cell differentiation ability was performed by differentiation media and supplements (Cyagen US Inc).

Preparation of exosomes

Healthy pregnant women umbilical cord collection from obstetrics of our hospital. We stated that the experiment process conform to the principles outlined in the declaration of Helsinki and investigators have obtained the informed written consent before enrolling participants in clinical trials. When reached 90% confluences, the adherent cells were incubated in medium with 5% exosome-depleted FBS for 24 h, and 5–8 passages hUCMSC were used for experiments. The conditioned medium was centrifuged at 4 °C at 300 g for 10 min at 2000 g for 10 min and finally at 10 000 g for 30 min to remove the cells and debris, followed by centrifugation of the supernatant at 100 000 g at 4 °C for 1 h. MSC-exo were resuspended in PBS and filtered with a 0.22 μm microfiltration membrane, centrifuged again in PBS at 100,000 g for 1 h to collect the exosomes. The protein concentration of hUCMSC-EXO was determined using a bicinchoninic acid (BCA) assay kit.

Characterization of MSC-EXO

Transmission electron microscope (TEM) was used to detection the morphology of MSC-EXO according to the manufacturer's instructions. Briefly, the prepared exosomes were stained with phosphotungstic acid solution and then performed under a Hitachi-9000 TEM system. The exosome markers CD63, CD81,TSG101ALIX and were analyzed by western blot.

Experimental design

We established rats PAH model through a single intraperitoneal injection of MCT(60 mg/kg; Sigma, St. Louis, MO, USA). Three weeks later, 25 μg/day or an equal volume of PBS, for 3 days starting 1 weeks after the last series MCT or vehicle injections[12]. The animals were randomly divided into 3 groups(n = 10): Control (saline-treated) group, MCT-PAH group, and MCT + EXO group. Four weeks after MCT injection, the rats were anesthetized with pentobarbital (30 mg/kg, ip, Sigma Aldrich) and inserted with a 3F-Miller micro-tip catheter via the right jugular vein into the right ventricle (RV) to obtain the right ventricular systolic pressure (RVSP).

Lung histology

Post-operation, the heart was obtained, and the weight ratio of the right ventricular (RV) to left ventricle (LV) plus the septum (LV + S) and the right ventricular weight was calculated to quantify the right ventricular hypertrophy. The lung tissues were fixed and embedded in paraffin, the serially sections at a thickness of 4–5 μm were stained with hematoxylin-eosin stain. The vascular wall thickness (WT), vascular external diameter (ED), vascular wall area (WA) and total vascular area (TA) to calculate WT% (WT/ED) and WA% (WA/TA) were measured as previously study. On the other hand, the serially sections were stained with Masson's trichrome to measure the evaluation the degree of fibrosis.

Immunohistochemistry and immunofluorescence

Immunohistochemistry and immunofluorescence were used to analysis the expression of CD31, a-SMA and V-Ecadherin. Briefly, after blocking with 5% bovine serum albumin for 30 min at room temperature, the lung sections were incubated overnight at 4 °C with anti-CD31 (AF3628), α-SMA (ab21027) and V-Ecadherin (CST#14472) antibodies. Then, sections were further incubated with a antibody for 2 h at room temperature. Subsequently, the 3, 3'- diaminobenzidine (DAB) dye was added to visualize the antibodies. For immunofluorescence, the sections were followed by 1-h incubation in the dark with florescence isothiocyanate-conjugated secondary antibody. Images were taken with ZEISS LSM800 confocal microscope (Tokyo, Japan). All experiments were performed by two examiners blinded to treatment assignment.

PAEC culture

Rats PAEC were purchased from Procell Life Science&Technology Co,.Ltd. (Wuhan, China), and cultured in special culture medium (Procell, China) supplemented with 100 Ug/ml of penicillin, 100 IU/ml streptomycin, and 10% (vol/vol) fetal bovine serum (FBS) at 37 °C in a humidified normoxia condition (21% O_2, 5% CO_2,74% N_2) or a hypoxia condition (3% O_2, 5% CO_2, 92% N_2). Cells were passaged after > 80% confluence, digested with 0.05% trypsin including 0.04% EDTA (Sigma-Aldrich, St. Louis, MO) in PBS. Cells were treatment with MSC-exo fraction (100 μg/ml) at 37 °C, respectively.

siRNA preparation

Here, the gene of Wnt5a was knocked down in PAEC by transfecting siRNA targeting. The siRNA oligonucleotides were selected to correspond to the nucleotide sequence of si-r-Wnt5a: 5'-GGACAACACTTCTGTCTTT-3'.Total RNA was extracted from cells using a Qiagen RNeasy kit (Qiagen, Basel, Switzerland). Complementary DNA (cDNA) first strand was produced using a Superscript first-strand synthesis system using oligo (dt) antisense primers (Invitrogen,Lucerne, Switzerland). Amplified fragments were analyzed in 1.5% agarose gelelectrophoresis in the presence of ethidium bromide (Sigma-Aldrich). GAPDH was used as an internal control for the amount of RNA input.

MTT assay and BrdU incorporation

To evaluate the survival rate of cells, PAECs were seeded into 96-well plates at about at a density of 5×10^3 cells/well. The cells were subjected to hypoxia 48 h with or without MSC-EXO. After that, cells were incubated with 3-(4,5-dimethylthiazol-2-yl)-2,5-diphenyltetrazolium bromide (MTT) at a concentration of 0.5% inmedium, at 37 °C for 4 hours. The absorbance was measured at 490 nm in a spectrophotometer.

The Bromodeoxyuridine (BrdU) incorporation assays were implemented according to the manufacturer's instructions. Briefly, Cultured PAEC in 96-well culture plates were incubated with 5-BrdU labeling solution for approximately 48 h, anti-BrdU monoclonal antibody was incubated for 1 hour, and goat anti-mouse IgG was conjugated. The absorbance of the sample was detected using a spectrophotometer microplate reader at at 450/550 nm.

Real-time PCR

Quantitative real-time polymerase chain reaction (qRT-PCR) analysis was performed to detect the relative expression of Bcl-2 BAx, Capase-3, CD31, a-SMA and V-Ecaherin using genespecific primers as described previously. Briefly, total RNA in lung tissues or PAEC in each group was extracted using RNeasy kit (Qiagen, Valencia, CA). ABI Prism 7900 sequence detection system software (version 2.2) was used to analysis the data were, and β-actin was used as an internal control for input RNA. The primers were designed by the Primer Express software package.

Western blot

Here, the antibodies of CD63 (Invitrogen,10628D), CD81(MA5-32333), TSG101(MA5-32463), CD31 (AF3628), α-SMA (ab21027), V-Ecadherin (CST#14472), Wnt5a (ab174963), Wnt11(ab31962), β-catenin (ab32572), Cyclin D1(MA5-15512) and PCNA(ab92552) were used respectively, overnight at 4 °C. The primary antibody-labeled membranes were then treated with the horseradish peroxidase (HRP)-conjugated goat anti-rabbit secondary antibody to IgG (ab205718) at room temperature for 1.5 h. GAPDH or β-actin expression was used as an internal control.

Scratch-wound assay

About 5×10^5 PAEC were plated onto 24-well plates, and were grown for 48 h to a confluence of > 90%. When the cells were stably transfected with Wnt5a and treated with or without 100 ng/ml MSC-EXO, and

then they were incubated for another 12 h. Scratch-wound assay was performed by manually scraping the cell monolayer with a 10-μl plastic pipette tip.

Cell migration assay

The migratory function of PAEC was measured by a modified Boyden chamber (Transwell; Corning Life Sciences, Inc., Tewksbury, MA, USA). In brief, cells in each group were treated with complete medium containing 1% FBS and were added into the upper chamber. The lower chamber was in the presence of 10% FBS. 48-h later, cells that had not migrated were removed, whereas migrated cells. And then they were fixed and stained with the Crystal Violet Staining Solution kit (Solarbio, Beijing Solarbio Science & Technology Co., Ltd., Beijing, China).

Statistical analysis

Data of continuous variables are presented as mean ± standard deviation (SD); while data not conforming to homogeneity of variance or normal distribution were expressed as interquartile range. Comparisons of mean values between two groups were analyzed using a non-paired t-test. Comparisons among multiple groups were analyzed by one-way analysis of variance (ANOVA), followed by Scheffe post hoc test test. Statistical analysis was carried out by using the SPSS 1.9 software (IBM, Armonk, NY, USA). $P < 0.05$ was regarded as significant statistical difference.

Results

Characterization and differentiation potential of hUCMSCs

The surface markers were determined by fluorescence activated cell sorting (FACS) showed that the majority of hUCMSCs expressed high levels of the CD73, CD90, and CD105 markers, whereas CD34, CD45 and HLA-DR markers were relatively absent (Figure 1A). On the other hand, according to the Alizarin Red-S, Oil Red-O and Toluidine blue staining, the cells had the ability to differentiate into osteocytes, adipocytes and cartilage (Figure1B).

Characterization of the shape and size of MSC-EXO derived from human umbilical cord was carried out by transmission electron microscope, as shown in Figure1C, the range of MSC-EXO was between 50-150 nm in size.The protein expression of MSC-EXO markers was detected by western blot, as shown in Figure1D, an enrichment of CD9, CD63, CD81, ALIX and TSG101 levels in MSC-EXO than MSC-CM. In order to identify whether the MSC-EXO released by MSCs could transfer to cells, the exosomes were traced by PKH67 and co-cultured with PAMSC, which was observed under a con-focal fluorescence microscopy at 0 h and 6 h after co-culture (Figure1E) .

Effect of MSC-EXO on monocrotaline-PAH and pulmonary vascular remodeling

Four weeks after MCT injection, our results showed that a significant decrease of RVSP and RV/(LV + S) in MSC-EXO administration rats than that in MCT-induced PAH rats (P<0.05; Figure 2A). On the other hand, WT% and MA% of muscular arteries were significantly increased in MCT group than in control, but notably decreased in MSC-EXO group (P<0.05; Figure 2A and 2B). Masson's trichrome staining results showed that there was obvious collagen deposition in the pulmonary interstitium in the MCT rats, but a significantly alleviated in the MSC-EXO treatment rats (Figure 2C). Immunohistochemical result showed that the expression of PAEC markers CD31 was significantly increased in MSC-EXO treatment group as compared with MCT group (Figure 2D). On the other hand, western blot result showed that the protein expression of PCNA was significantly reduced in MSC-EXO group than that in MCT group (P <0.05, Figure 2E).

Effects of MSC-EXO on MCT-induced endothelial-to-mesenchymal transition

We used double immunofluorescence staining for CD31, α-SMA and V-Ecadherin to determine whether MSC-EXO treatment reduced MCT-indiced endothelial-to-mesenchymal transition (EndMT) in pulmonary vascular. The results showed that the expression of CD31 and V-Ecadher was significantly decreased, but a significantly increased expression of α-SMA in MCT-rats, indicating EndMT was induced in the process of MCT-triggered PAH. However, a obviously restored expression in MSC-EXO treatment group (Figure 3A and 3B). On the other hand, the gene and protein of CD31,V-Ecadherin and a-SMA were exaltation by qRT-PCR and western blot, the results showed that mRNA and protein expression of CD31 and V-Ecadherin were significantly increased, respectively, but a significant decreased of α-SMA expression in MSC-EXO treatment group that MCT group (P<0.01, Figure 3C and 3D).

Effect of MSC-exo on apoptosis in and Wnt/BMP signaling pathway

The MCT-induced cells apoptosis was observed by analysis the mRNA and protein expression levels of antiapoptotic gene Bcl2, the proapoptotic genes caspase-3 and Bax. The results showed that as compared with MSC-PAH group, Bcl2 was significantly decreased, but caspase-3 and Bax were significantly increased in MSC-EXO group (P<0.01, Figure 4A and 4B).

The protein expression levels of Wnt5a, Wnt 11, β-catenin and cyclin D1 were detected by western blot to further reveal the mechanism. We found that the levels of Wnt5a and Wnt11 were significantly decreased, but β-catenin and cyclin D1 levels were increased in MCT-PAH group than that in the control; however, these results were significantly reverse in MSC-EXO treatment group (P<0.05, Figure 4C). These results suggest that MSC-EXO attenuate PAH pulmonary vascular remodeling maybe through regulation of Wnt5/β-catenin signal pathway.

Moreover, the expression of BMP signaling axis molecules were determined in the present study.The results indicated that the protein expression of BMPR2 and Smad1/5/8 were obviously higher, but Smad 2/3 was lower in MSC-EXO group than that in MCT-PAH group (P<0.05, Figure 4D). These results showed that MSC-EXO inhibited MCT-PAH pulmonary vascular remodeling was also through regulation of BMP signaling pathways.

Effect of MSC-EXO on hypoxia-induced PAECs injury in *vitro*

The protein expression of Wnt5a signaling pathway in hypoxia-PAEC were also measured by western blot. Th results showed that when the cells were hypoxia exposure for 72 h, the expression of Wnt5a were significantly decreased in hypoxia-induced PAEC, however, this reduction was restored in MSC-EXO group (P<0.05, Figure 5A).

To investigate the role of Wnt5a pathway in MSC-EXO against hypoxia-induced cell damage, Wnt5a was knocked down by transfecting siRNA targeting Wnt5a. As showen in Figure 5B, transfection of Wnt5a siRNA caused a reduction in Wnt5a expression and the inhibition efficacy was about 97.4 % at mRNA level, 70.4% at protein level in PAEC, respectively(P<0.05).

Effect of MSC-EXO on hypoxia-induced PAEC proliferation

The MTT and BrdU incorporation assay results indicated that the PAEC viability and proliferation was significantly reduced in MSC-EXO group as compared with hypoxic exposure group(P<0.05, Figure 6A and 6B). To further analysis the proliferation, the protein expression of PCNA and Ki67 was detected by western blot and immunofluorescence. Which showed that the level of PCNA was obviously decreased after the cell culture together with MSC-EXO group as compared with hypoxia group (P<0.05, Figure 6C). Immunofluorescence staining with Ki67 antigen results showed that the expression of Ki67 was substantially decreased in MSC-EXO group as compared with hypoxia group (P<0.05, Figure 6D). The above results were significantly inhibited by siRNA transfection (P<0.05,).

On the other hand, the wound healing and Transwell assays results showed the invasion and migration ability of the hypoxia-PAECs was significantly inhibited after treatment of the cells with MSC-EXO (P<0.05, Figure 7A and 7B). The above results were significantly inhibited by siRNA transfection (P<0.05).

Effect of MSC-EXO on BMPR2 pathway in hypoxia-induced PAEC

Here, the protein expression of BMP and Wnt5a signaling pathways related molecules was detected to evaluation the interaction between BMP and Wnt signaling was evaluated in *vitro.* The results indicated that the protein expression of BMPR2 and Smad1/5/8 were obviously higher, but Smad 2/3 was lower in

MSC-EXO group than that in MCT-PAH group (P<0.05, Figure 3D). However, when the cells were transfection with Wnt5a siRNA, the protein expression of BMPR2 signaling pathway was reversed (P<0.05, Figure 7C).

In order to observe the effect on hypoxic-induced cells adhesion and contraction, the protein expression of endothelial cells marker CD31, smooth muscle cells markers -SMA and adherens junctions protein of V-Ecadherin were measured by immunofluorescence and western blot. The results showed that the levels of CD31 and V-Ecadherin were significantly higher, α-SMA was significant lower in MSC-EXO group than that in hypoxia group (P<0.05, Figure 8A and 8B). Furthermore, these results wrere also be reversed after cells were transfection with Wnt5a siRNA, The above data suggested that the inhibition effect on EndMT and promotion adhesion ability of MSCEO may be associated with regulation Wnt5a/BMPR2 signaling pathway.

Discussion

Our present study data demonstration that administration of MSC-EXO derived from human umbilical cord MSCs (hUCMSCs) could significantly inhibit MCT-induced pulmonary arterial hypertension (PAH) vascular remodeling, reduce the right ventricular hypertrophy, and suppress the progression of endothelial-to-mesenchymal transition (EndMT) via regulating Wnt5a/BMP signaling pathway.

Wingless (Wnt) signaling pathway is divided into canonical signaling pathway and non-canonical signaling pathway. The endothelial cells (ECs) through the non-canonical Wnt ligands in a short-range, paracrine manner stable connection in vascular remodeling. Loss of Wnt5a or Wnt11 derived from endothelin will let ECs polarization direction against the blood flow direction in the low wall shear stress[13,14]. A large number of evidence indicated that Wnt5a involved in the pathogenesis of PAH[1.9.15], which has the role of regulating human endothelial cell proliferation and migration through noncanonical signaling [16,17] and inhibiting hypoxia-induced PASMC proliferation via suppression of of β1-catenin/cyclin D1. Here, our present study showed that the expression of Wnt5a was significantly increased, β-catenin and cyclin D1 were decreased in MSC-EXO group as compared with MCT or hypoxia group in *vivo* or *vitro*. Reports showed that the pulmonary vascular cell proliferation induced by hypoxia was accompanied by the increase of Cyclin D1 and β-catenin expression, and further activation many transcription activation. To determine whether Wnt5a plays an active role in proliferation of hypoxia-PAEC, we examined proliferation after manipulation of Wnt5a expression. We found that knockdown of Wnt5a could inhibited hypoxia-induced proliferation of PAEC. The present study indicated that MSC-EXO could attenuate PAH pulmonary vascular remodeling via regulation of Wnt5a/β-catenin and its target gene Cyclin D1.

Although the production of Wnt5a is regarded as a potential treatment for PAH, still there are some limitations. Such as possible involvement of other Wnt pathways was not investigated. Bone morphogenetic proteins (BMPs) and their receptors were required for PAH vascular remodeling. More than 70% of heritable cases of PH and approximately 20% of apparently sporadic cases of idiopathic PAH has

II type BMP receptor (BMPR2) gene mutation [18]. BMP signaling pathways has an important role in the regulation of cell proliferation, migration, differentiation and apoptosis, these are the key factors in vascular remodeling [19]. BMPs signaling could stimulate activation of SMAD transcription factors through heteromeric receptor complexes [20]. Inhibition of BMP/SMAD signaling directly leads to a reduction in SMAD1/5/8 pathway and to a concomitant increase in SMAD2/3 pathway, and change the gene transcription regulation of the pulmonary fibrosis occurrence [21]. Reduced BMPR2 expression can also impair PAECs function including influence apoptosis and tube formation, promote PASMCs proliferation[22,23]. The present study showed that injection of MSC-EXO could obviously increase BMPR2 expression than that in MCT-PAH rats. A recent study reports that interaction between BMP and Wnt closely associated with lung development, those cascade coordination regulation stem cell fate which determine lung branching morphogenes[18]. BMPR2 promotes PAEC proliferation, survival, and motility by recruiting Wnts to support normal PAEC function. Therefore, whether the interaction of Wnt5a and BMPR2 are involved in MSC-EXO inhibition of pulmonary hypertension, it still needs further research. In our study, we observed the effect of MSC-EXO on BMPR2 expression when Wnt5a gene was silence in hypoxia-PAEC. Our results showed that BMPR2 was significantly increased in MSC-EXO group than that in hypoxia groups, however, it was significantly decreased in Wnt5a siRNA groups. These results suggested that MSC-EXO inhibition PAH pulmonary vascular remodeling maybe through regulating the interaction of Wnt and BMP signaling pathway.

The potential role of EndMT in vascular remodeling and the fibrotic lung disease haas also been reported[31-34]. ECs undergoing EndMT lose their surface marker protein, such as CD31 and vascular endothelial cadherin (V-Ecadherin), but acquire mesenchymal phenotype α-SMA. Reports showed that EndMT partially increased was associated with lower BMPR2 expression [24-27]. In the present study, we also observed the effect of MSC-EXO on EndMT, the results showed that CD31 and V-Ecadherin were significant higher, but α-SMA expression was lower in MSC-EXO group as compared with MCT-induced PAH or hypoxia-PAEC groups. These results indicated that MSC-EXO reduced PAH vascular remodeling was through regulation of BMP signaling pathway related of EndMT. On the other hand, non-canonical Wnt signaling through regulation of cell migration and cell polarity to control vascular remodeling[28]. Wnt5a helps cells to move together by stabilizing vinculin at cell junctions and play an important role in endothelial cell migration[17]. Reports showed that V-Ecadherin was an important factor in cells junctions [29-32]. V-Ecadherin associated with endothelial polarity in collective migration, and Wnt non-canonical signaling through coordination cells cohesion balance net movement[33-35]. Furthermore, our results showed that siRNAWnt5a transfection could reverse the expression of V-Ecadherin. Taken-together, in the present study, our results suggested that MSC-EXO inhibit PAH vascular remodeling maybe through regulating Wnt5a and/or BMPR2 signaling pathway and then up-regulation V-Eadherin expression, the mechanism needs further research.

Conclusion

In summary, the present study showed for the first time that MSC-EXO increased the expression of Wnt5a further to regulation BMPR2 signaling pathway to prevention and treatment of PAH vascular remodeling.

Those can not be clarified in the present study and would need further investigations.

Abbreviations

BMPR2: II type BMP receptor; EndMT: Endothelial-to-mesenchymal transition; EXO: Exosomes; hUCMSCs: Human umbilical cord mesenchymal stem cells; LV+S:Left ventricular plus septal weight; MCT: Monocrotaline; PAEC: Pulmonary arterial endothelial cell; PASMC: Pulmonary arterial smooth muscle cells; PH: Pulmonary hypertension; RVSP: Right ventricular systolic pressure; RT-PCR: Real-time polymerase chain reaction; Wnt: Wingless

Declarations

Acknowledgements

The authors are grateful to the Central Research Laboratory of the Second Hospital of Shandong University for technical assistance and generous support.

Authors' contributions

Experimental Design: YL; Experiments: SSZ, LLG, ZHZ, CYX, JW, WJ and QX; Data analysis: YL, SSZ and LLG. All authors read and approved the final manuscript.

Funding

This project was supported by the Science and Technology Development Project of Jinan Medical and Health (201907001), the Science and Technology Development Project of Shandong Province (2019GSF107093, 2019GSF108198, 2018GSF118106), Youth Interdisciplinary Innovation Science Fund of Shandong University (2020QNQT019), and the Scientific and Development Funds of the Second Hospital of Shandong University (26010232007005).

Availability of supporting data

All data generated in this study are included in this manuscript.

Ethical Approval and Consent to participate

All participants were provided with written informed consent at the time of recruitment. And this study was approved by the Ethics Committee of the Second Hospital of Shanodng University.

Consent for publication

Not applicable.

Competing interests

The authors declare that they have no competing interests.

References

1. Yuan K, Shamskhou EA, Orcholski ME, Nathan A, Reddy S, Honda H, Mani V, Zeng Y, Ozen MO, Wang L, Demirci U, Tian W, Nicolls MR, de Jesus Perez VA. Loss of Endothelium-Derived Wnt5a Is Associated With Reduced Pericyte Recruitment and Small Vessel Loss in Pulmonary Arterial Hypertension. Circulation. 2019;139:1710-1724.
2.MMP-2 and MMP-9 contribute to the angiogenic effect produced by hypoxia/15-HETE in pulmonary endothelial cells.Liu Y, Zhang H, Yan L, Du W, Zhang M, Chen H, Zhang L, Li G, Li J, Dong Y, Zhu D.J Mol Cell Cardiol. 2018 ;121:36-50.
3.Singh N, Singh H, Jagavelu K, Wahajuddin M, Hanif K. Fatty acid synthase modulates proliferation, metabolic functions and angiogenesis in hypoxic pulmonary artery endothelial cells. Eur J Pharmacol. 2017;815:462-469.
4.Teichert-Kuliszewska K, Kutryk MJ, Kuliszewski MA, Karoubi G, Courtman DW, Zucco L, Granton J, Stewart DJ.Bone morphogenetic protein receptor-2 signaling promotes pulmonary arterial endothelial cell survival: implications for loss-of-function mutations in the pathogenesis of pulmonary hypertension. Circ Res. 2006;98(2):209-17.
5. Huertas A, Perros F, Tu L, Cohen-Kaminsky S, Montani D, Dorfmüller P, Guignabert C, Humbert M. Immune dysregulation and endothelial dysfunction in pulmonary arterial hypertension: a complex interplay. Circulation. 2014;129(12):1332-40.
6.Rabinovitch M, Guignabert C, Humbert M, Nicolls MR.Inflammation and immunity in the pathogenesis of pulmonary arterial hypertension. Circ Res. 2014;115(1):165-75.
7.Takahashi J, Orcholski M, Yuan K, de Jesus Perez V. PDGF-dependent β-catenin activation is associated with abnormal pulmonary artery smooth muscle cell proliferation in pulmonary arterial hypertension.FEBS Lett. 2016;590(1):101-9.
8.Yu XM, Wang L, Li JF, Liu J, Li J, Wang W, et al.Wnt5a inhibits hypoxia-induced pulmonary arterial smooth muscle cell proliferation by downregulationof β-catenin. Am J Physiol Lung Cell Mol Physiol. 2013;304(2):L103-11.
9.Aliotta JM, Pereira M, Wen S, Dooner MS, Del Tatto M, Papa E, Goldberg LR, Baird GL, Ventetuolo CE, Quesenberry PJ, Klinger JR.Exosomes induce and reverse monocrotaline-induced pulmonary hypertension in mice. Cardiovasc Res. 2016 1;110(3):319-330.
10.Lee C, Mitsialis SA, Aslam M, Vitali SH, Vergadi E, Konstantinou G, Sdrimas K, Fernandez-Gonzalez A, Kourembanas S. Exosomes mediate the cytoprotective action of mesenchymal stromal cells on hypoxia-induced pulmonary hypertension. Circulation. 2012;126(22):2601-2611.
11.Hogan SE, Rodriguez Salazar MP, Cheadle J, Glenn R, Medrano C, Petersen TH, Ilagan RM. Mesenchymal stromal cell derived exosomes improve mitochondrial health in pulmonaryarterial hypertension. Am J Physiol Lung Cell Mol Physiol. 2019;316(5):L723-L737.
12.Aliotta JM, Pereira M, Amaral A, Sorokina A, Igbinoba Z, Hasslinger A, et al. Induction of pulmonary hypertensive changes by extracellular vesicles from monocrotaline-treated mice.Cardiovasc Res.

2013;100(3):354-62.
13.Murphy N, Gaynor KU, Rowan SC, Walsh SM, Fabre A, Boylan J, et al. Altered expression of bone morphogenetic protein accessory proteins in murine and human pulmonary fibrosis.Am J Pathol 2016;186(3):600-15.
14.Franco CA, Jones ML, Bernabeu MO, Vion AC, Barbacena P, Fan J, Mathivet T, Fonseca CG, Ragab A, Yamaguchi TP, Coveney PV, Lang RA, Gerhardt H. Non-canonical Wnt signalling modulates the endothelial shear stress flow sensor in vascular remodelling.Elife. 2016;5:e07727.
15.Jin Y, Wang W, Chai S, Liu J, Yang T, Wang J.Wnt5a attenuates hypoxia-induced pulmonary arteriolar remodeling and right ventricular hypertrophy in mice. Exp Biol Med (Maywood) 2015;240(12):1742-51.
16. Konigshoff M, Eickelberg O.Wnt signaling in lung disease: a failure or a regeneration signal? Am J Respir Cell Mol Biol 2010,42(1):21-31.
17.Vuga LJ, Ben-Yehudah A, Kovkarova-Naumovski E, Oriss T, Gibson KF, Feghali-Bostwick C, et al. WNT5A is a regulator of fibroblast proliferation and resistance to apoptosis. Am J Respir Cell Mol Biol 2009,41(5):583-9.
18.Tu L, Desroches-Castan A, Mallet C, Guyon L, Cumont A, Phan C, Robert F, Thuillet R, Bordenave J, Sekine A, Huertas A, Ritvos O, Savale L, Feige JJ, Humbert M, Bailly S, Guignabert C.Selective BMP-9 Inhibition Partially Protects Against Experimental Pulmonary Hypertension.Circ Res. 2019 Mar 15;124(6):846-55.
Liu Y, Zhang H, Yan L, Du W, Zhang M, Chen H, Zhang L, Li G, Li J, Dong Y, Zhu D. MMP-2 and MMP-9 contribute to the angiogenic effect produced by hypoxia/15-HETE in pulmonary endothelial cells. J Mol Cell Cardiol. 2018;121:36-50.
19.Morrell NW, Bloch DB, ten Dijke P, Goumans MJ, Hata A, Smith J, Yu PB, Bloch KD. Targeting BMP signaling in cardiovascular disease and anaemia. Nat Rev Cardiol. 2016; 13(2):106-20.
20.Long L, Ormiston ML, Yang X, Southwood M, Gräf S, Machado RD, Mueller M, Kinzel B, Yung LM, Wilkinson JM, Moore SD, Drake KM, Aldred MA, et al. Selective enhancement of endothelial BMPR-II with BMP9 reverses pulmonary arterial hypertension. Nat Med. 2015; 21(2):777-85.
21.Wu FJ, Lin TY, Sung LY, Chang WF, Wu PC, Luo CW. BMP8A sustains spermatogenesis by activating both SMAD1/5/8 and SMAD2/3 in spermatogonia. Sci Signal. 2017;10(477).
22.Nie X, Tan J, Dai Y, Liu Y, Zou J, Sun J, et al. CCL5 deficiency rescues pulmonary vascular dysfunction, and reverses pulmonary hypertension via caveolin-1-dependent BMPR2 activation. J Mol Cell Cardiol 2018;116:41-56.
23.Gomez-Puerto MC, van Zuijen I, Huang CJ, Szulcek R, Pan X, van DintherMA, et al. Autophagy contributes to BMP type 2 receptor degradation and development of pulmonary arterial hypertension.J Pathol 2019;249(3):356-67.
24.Reynolds AM, Holmes MD, Danilov SM, Reynolds PN. Targeted gene delivery of BMPR2 attenuates pulmonary hypertension. Eur Respir J. 2012;39:329-43.
25.Arciniegas E, Frid MG, Douglas IS, Stenmark KR. Perspectives on endothelial-to-mesenchymal transition: potential contribution to vascular remodeling in chronic pulmonary hypertension. Am J Physiol Lung Cell Mol Physiol. 2007;293:L1–L8.
26.Cheng SL, Shao JS, Behrmann A, Krchma K, Towler DA. Dkk1 and MSX2-Wnt7b signaling reciprocally

regulate the endothelial-mesenchymal transition in aortic endothelial cells. Arterioscler Thromb Vasc Biol. 2013;33:1679–89.
27.Willis BC, Borok Z. TGF-beta-induced EMT: mechanisms and implications for fibrotic lung disease. Am J Physiol Lung Cell Mol Physiol. 2007;293:L525-L534.
28.Korn C, Scholz B, Hu J, Srivastava K, Wojtarowicz J, Arnsperger T, et al. Endothelial cell-derived non-canonical Wnt ligands control vascular pruning in angiogenesis.Development 2014;141(8):1757-66.
29.Sauteur L, Krudewig A, Herwig L, Ehrenfeuchter N, Lenard A, Affolter M, Belting H-G. Cdh5/VE-cadherin promotes endothelial cell interface elongation via cortical actin polymerization during angiogenic sprouting. Cell Reports 2014;9:504-13
30.Bentley K, Franco CA, Philippides A, Blanco R, Dierkes M, Gebala V, Stanchi F, Jones M, Aspalter IM, Cagna G, Westro m S, Claesson-Welsh L, Vestweber D, Gerhardt H.The role of differential VE-cadherin dynamics in cell rearrangement during angiogenesis. Nature Cell Biology 2014; 16:309-21.
31.Ehling M, Adams S, Benedito R, Adams RH. Notch controls retinal blood vessel maturation and quiescence. Development 2013;140:3051-61.
32.Lobov IB, Cheung E, Wudali R, Cao J, Halasz G, Wei Y, Economides A, Lin HC, Papadopoulos N, Yancopoulos GD, Wiegand SJ. The Dll4/Notch pathway controls postangiogenic blood vessel remodeling and regression by modulating vasoconstriction and blood flow. Blood 2011; 117:6728-37.
33.Lobov IB, Cheung E, Wudali R, Cao J, Halasz G, Wei Y, Economides A, Lin HC, Papadopoulos N, Yancopoulos GD, Wiegand SJ. The Dll4/Notch pathway controls postangiogenic blood vessel remodeling and regression by modulating vasoconstriction and blood flow. Blood 2011; 117:6728-37.
34.Conway DE, Breckenridge MT, Hinde E, Gratton E, Chen CS, Schwartz MA. Fluid shear stress on endothelial cells modulates mechanical tension across VE-cadherin and PECAM-1. Current Biology 2013; 23:1024-30.
35.Vitorino P, Meyer T. Modular control of endothelial sheet migration. Genes & Development 2008;22:3268-81.

Figures

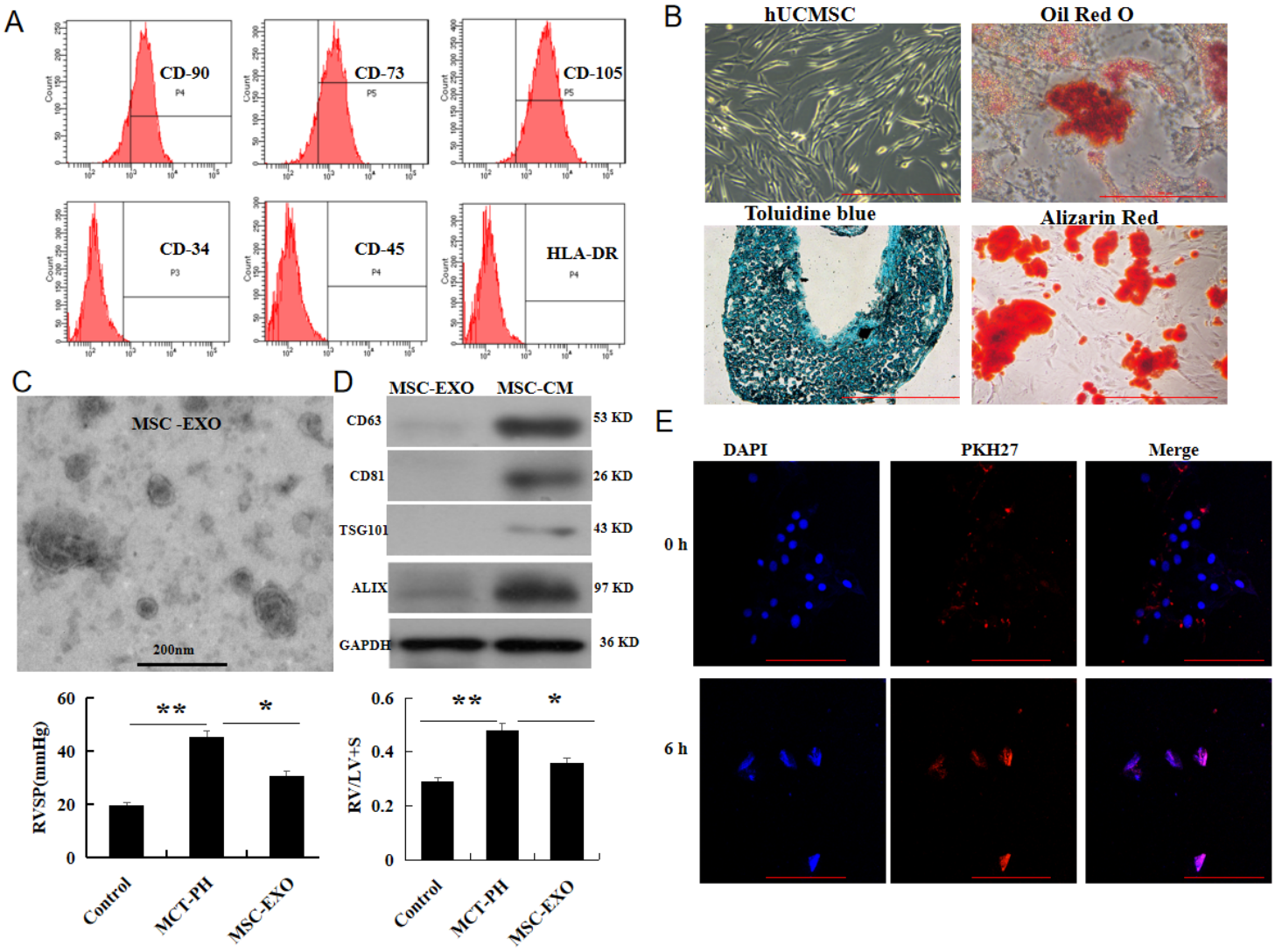

Figure 1

Characterization of human umbilical cord MSCs and MSC-EXO. (A) Surface marker analysis by flow cytometry. (B) Morphology and differentiated of MSCs into adipocytes, cartilage and osteocytes. (C) Transmission electron mcroscopy analysis. (D) The protein content of these MSC-EXO analyzed by western blot. (E) PKH-67 labeling. Red bar= 100 μm.

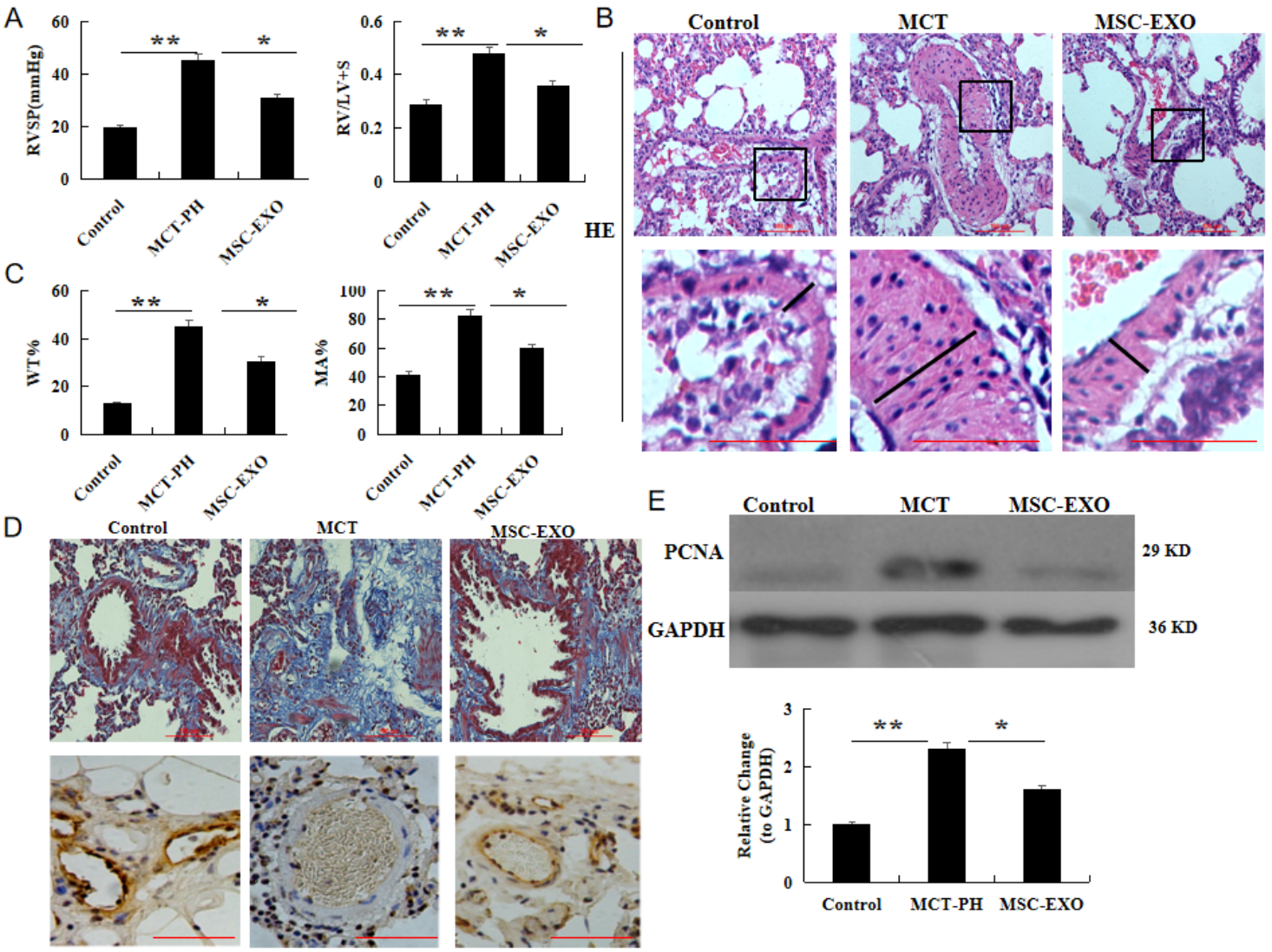

Figure 2

Effect of MSC-EXO on MCT-induced pulmonary artery pressure and vascular remodeling. (A) Comparative analysis of RVSP and RV/(LV+S) ratios (B) Representative hematoxylin and eosin staining images in each group. (C)Comparative analysis of the percent of wall thickness and wall area. (D) Massons staining. (E) CD31 in lung was detected by immunohistochemistry. (F) Proliferating cell nuclear antigen (PCNA) detected by western blot. n=10 rats per group; P<0.05, t-test; the data are present as mean ± SD; *MCT vs. control; #MSC-EXO vs. MCT group; Red bar= 100 μm.

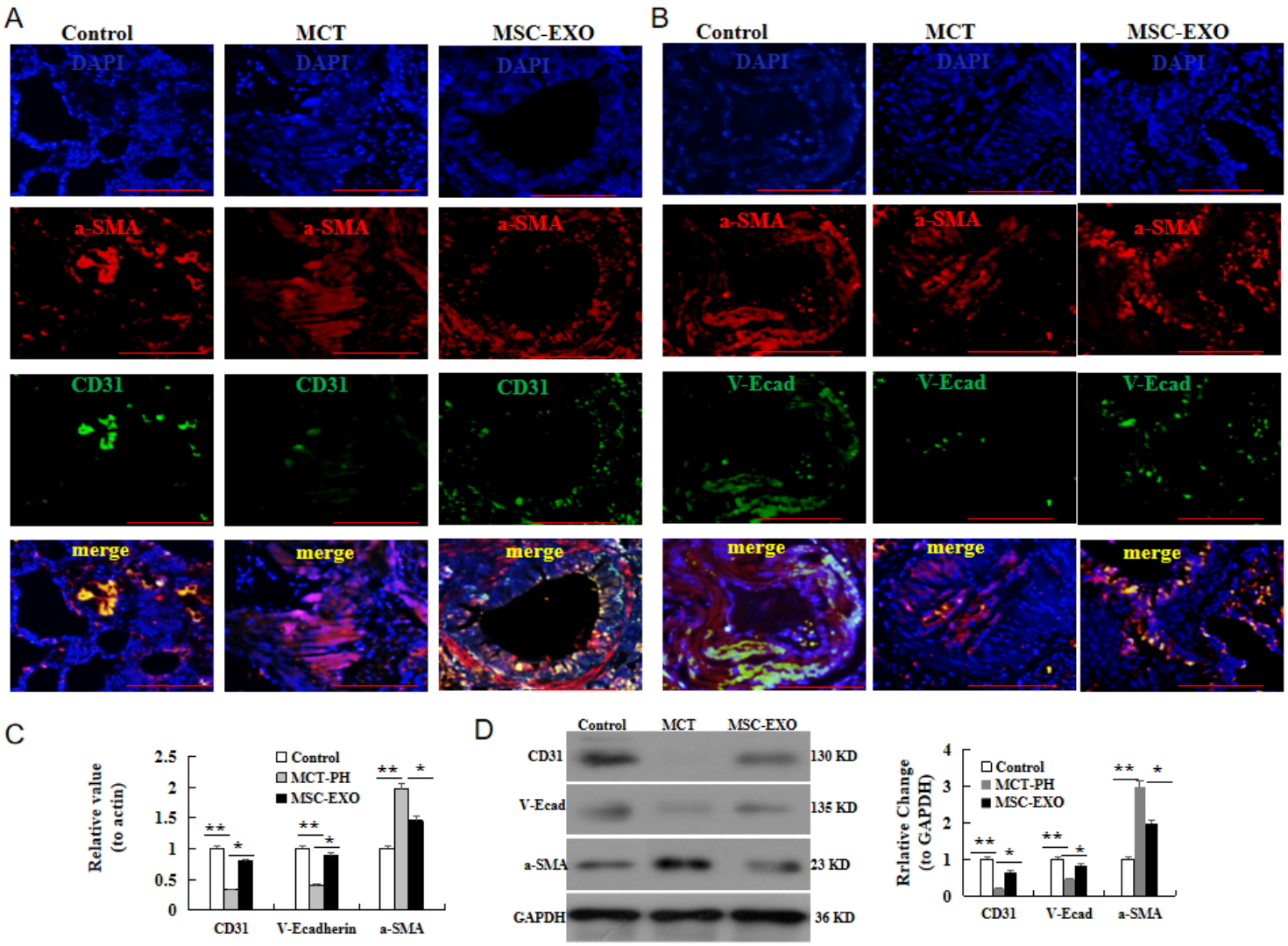

Figure 3

Effects of MSC-EXO on endothelial-to-mesenchymal transition in lungs. (A) Immunofluorescence staining with a-SMA (Red), CD31 (green) and the cell nuclei were labeled with DAPI (blue) in the pulmonary arterioles. (B) Immunofluorescence staining with a-SMA (Red), V-Ecadherin (green) and the cell nuclei were labeled with DAPI (blue). (C) Comparative analysis of mRNA level of a-SMA, CD31 and V-Ecadherin. (D) Protein expression of a-SMA, CD31 and V-Ecadherin analysis by western blot. n=10 rats per group; P<0.05, t-test; the data are present as mean ± SD; *MCT vs. control; #MSC-EXO vs. MCT group.

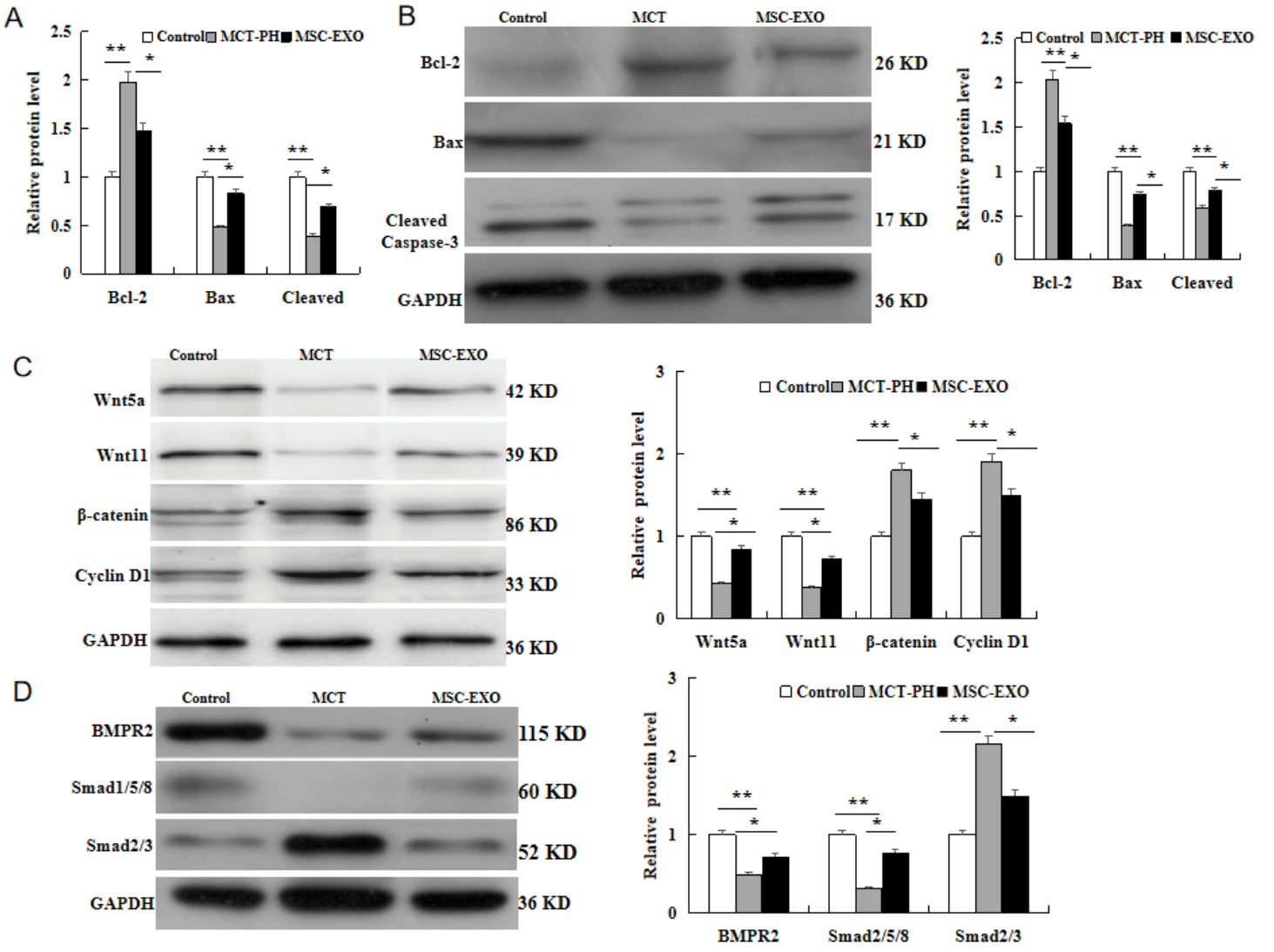

Figure 4

Apoptosis and Wnt/BMPR2 signaling pathway analysis in MCT-PAH. (A) comparative analysis of Bcl2, Bax and caspase-3 by RT-PCR. (B) Protein expression and comparative analysis of Bcl2, Bax and Cleaved caspase-3 by western blot. (C) Protein expression and comparative analysis of Wnt5a, Wnt11, β-catenin and Cyclin D1 by western blot. (D) BMPR2, Smad1/5/8 and Smad2/3 expression analysis by western blot. n=10 rats per group; P<0.05, t-test; the data are present as mean ± SD; *MCT vs. control; #MSC-EXO vs. MCT group.

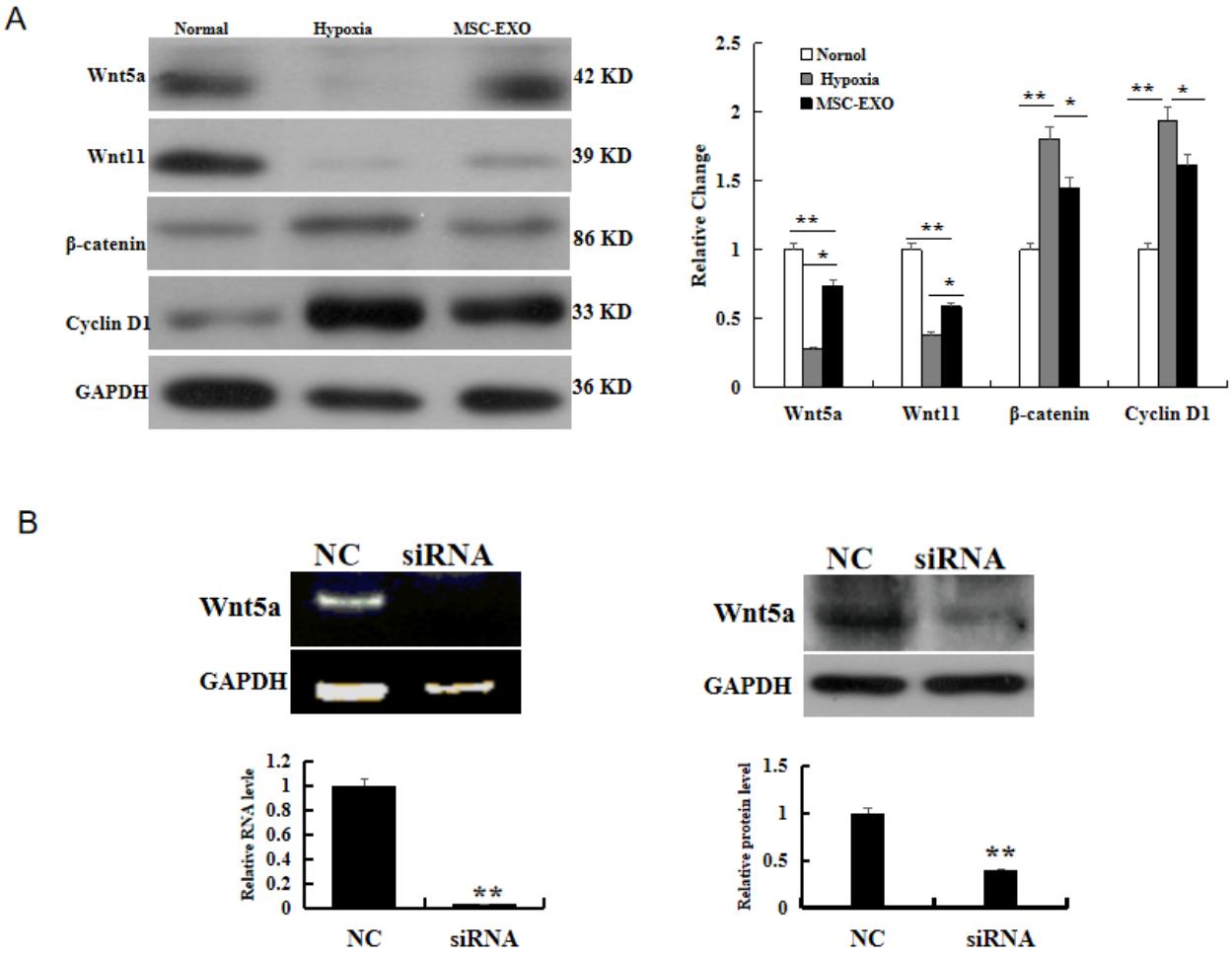

Figure 5

Effect of MSC-EXO on Wnt signaling pathway in vitro. (A) Protein expression and comparative analysis of Wnt5a, Wnt11, β-catenin and Cyclin D1 in hypoxia PAEC by western blot. (C) siRNA Wnt5a targeting transfecting analysis in PAECs by PCR and western blot. n=3 times repeated; P<0.01, t-test; the data are present as mean ± SD; **siRNA vs. Normal.

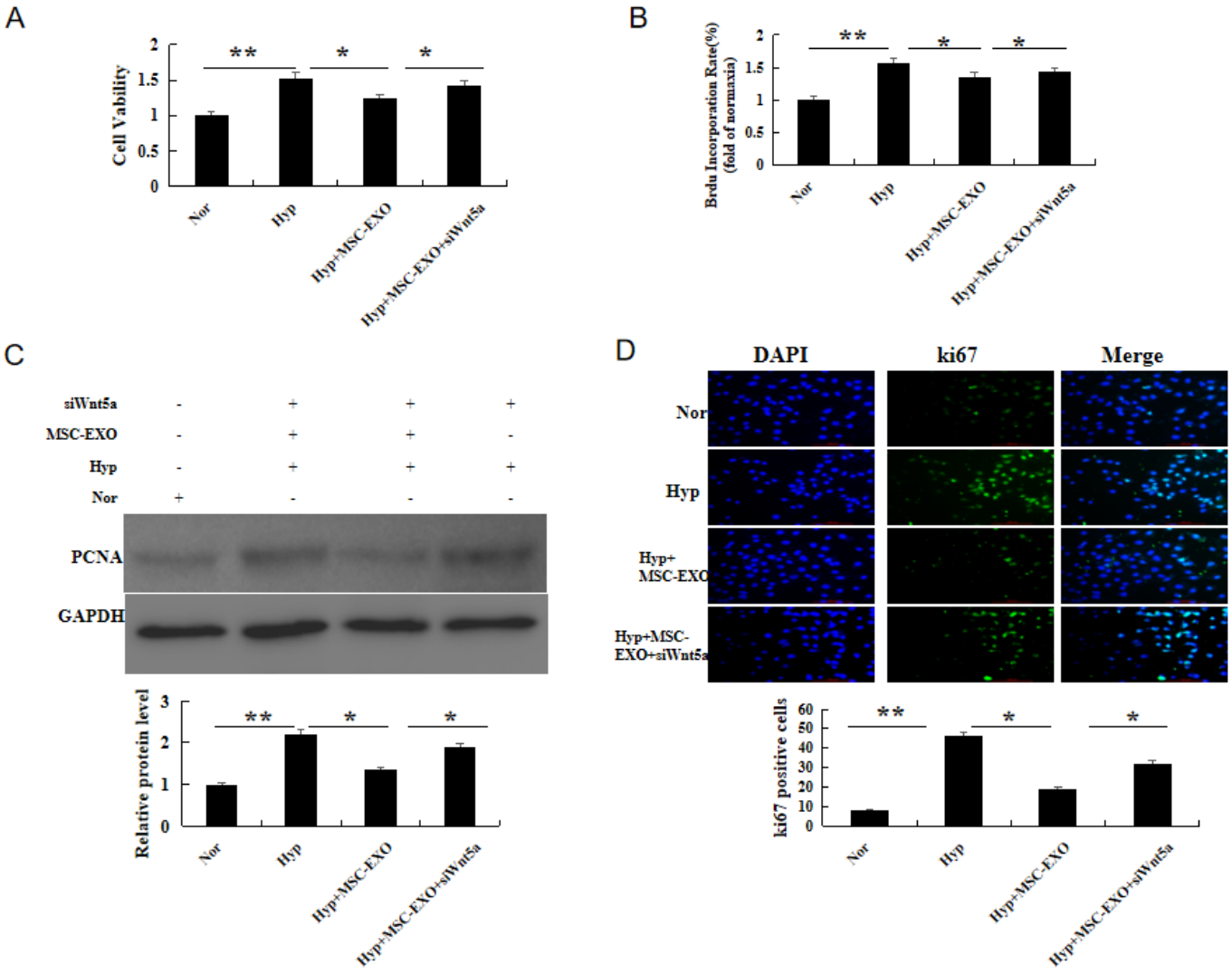

Figure 6

Effect of MSC-EXO on hypoxia-induced viability and proliferation in hypoxia PAEC. (A) Viability analysis by MTT. (B) Proliferation analysis by BrdU cell proliferation assay. (D) Protein expression and comparative of proliferating cell nuclear antigen (PCNA). (C) Immunofluorescence staining with Ki67 antigen. n=3 times repeated; P<0.05, one-way ANOVA followed by post hoc test; the data are present as mean ± SD; *hypoxia vs. control; #MSC-EXO vs. hypoxia group; * si Wnt5a vs. MSC-EXO group.

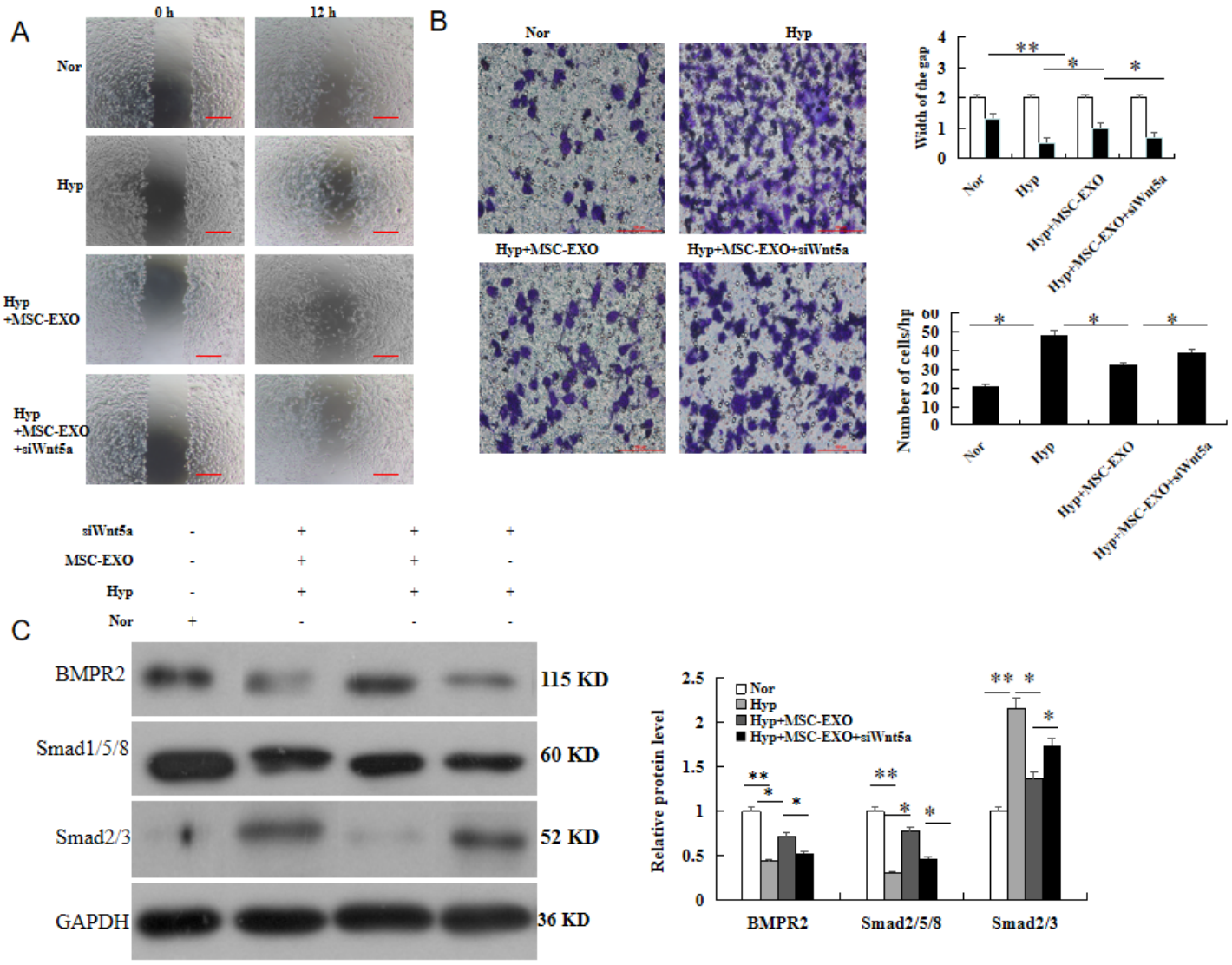

Figure 7

Effect of MSC-EXO on cells invasion, migration ability and BMPR2 signaling pathway analysis. (A)Wound healing and Transwell urinalysis. (B) Comparative of the invasion and migration ability. (C)Protein expression and comparative of BMPR2, Smad1/5/8 and Smad2/3. n=3 times repeated; P<0.05, one-way ANOVA followed by post hoc test; the data are present as mean ± SD; *hypoxia or vs. control; #MSC-EXO vs. hypoxia group; *siWnt5a vs. MSC-EXO group.

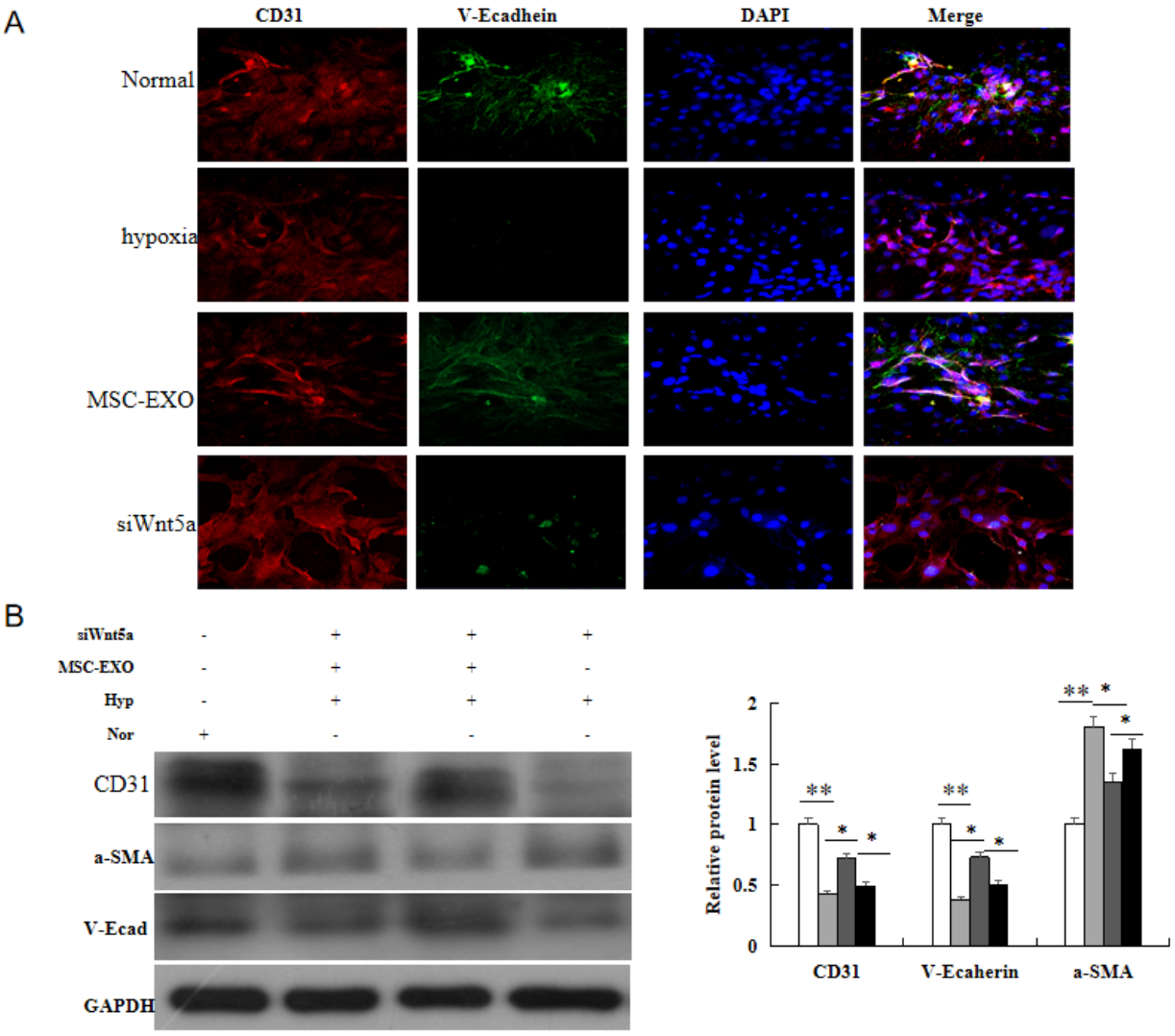

Figure 8

Effect of MSC-EXO on hypoxia-induced EndMT in PAECs. (A) Immunofluorescence analysis of CD31 and V-Ecadherin. (B) Protein expression and comparative analysis by western blot. n=3 times repeated; P<0.05, one-way ANOVA followed by post hoc test; the data are present as mean ± SD; *hypoxia or vs. control; #MSC-EXO vs. hypoxia group; *siWnt5a vs. MSC-EXO group.